



The two-dimensional kinetic ballooning theory for ion temperature gradient mode in tokamak

Cite as: Phys. Plasmas **24**, 102506 (2017); <https://doi.org/10.1063/1.5003652>

Submitted: 17 March 2017 . Accepted: 01 September 2017 . Published Online: 22 September 2017

T. Xie , Y. Z. Zhang, S. M. Mahajan, S. L. Hu , Hongda He, and Z. Y. Liu



View Online



Export Citation



CrossMark

ARTICLES YOU MAY BE INTERESTED IN

[The sensitivity of tokamak magnetohydrodynamics stability on the edge equilibrium](#)

Physics of Plasmas **24**, 102503 (2017); <https://doi.org/10.1063/1.4986036>

[Hall effect on tearing mode instabilities in tokamak](#)

Physics of Plasmas **24**, 102510 (2017); <https://doi.org/10.1063/1.5004430>

[Zonal flows driven by the turbulent energy flux and the turbulent toroidal Reynolds stress in a magnetic fusion torus](#)

Physics of Plasmas **24**, 102508 (2017); <https://doi.org/10.1063/1.5004555>



ULVAC

Leading the World with Vacuum Technology

- Vacuum Pumps
- Arc Plasma Deposition
- RGAs
- Leak Detectors
- Thermal Analysis
- Ellipsometers

The two-dimensional kinetic ballooning theory for ion temperature gradient mode in tokamak

T. Xie,^{1,a)} Y. Z. Zhang,² S. M. Mahajan,³ S. L. Hu,⁴ Hongda He,⁴ and Z. Y. Liu⁵

¹Department of Physics, Sichuan University of Science and Engineering, Zigong, Sichuan 643000, China

²Center for Magnetic Fusion Theory, CAS, Hefei, Anhui 230026, China

³Institute for Fusion Studies, University of Texas at Austin, Austin, Texas 78712, USA

⁴Southwestern Institute of Physics, P.O. Box 432, Chengdu, Sichuan 610041, China

⁵Department of Modern Physics, University of Science and Technology of China, Hefei, Anhui 230026, China

(Received 17 March 2017; accepted 1 September 2017; published online 22 September 2017)

The two-dimensional (2D) kinetic ballooning theory is developed for the ion temperature gradient mode in an up-down symmetric equilibrium (illustrated via concentric circular magnetic surfaces). The ballooning transform converts the basic 2D linear gyro-kinetic equation into two equations: (1) the lowest order equation (ballooning equation) is an integral equation essentially the same as that reported by Dong *et al.*, [Phys. Fluids B **4**, 1867 (1992)] but has an undetermined Floquet phase variable, (2) the higher order equation for the rapid phase envelope is an ordinary differential equation in the same form as the 2D ballooning theory in a fluid model [Xie *et al.*, Phys. Plasmas **23**, 042514 (2016)]. The system is numerically solved by an iterative approach to obtain the (phase independent) eigen-value. The new results are compared to the two earlier theories. We find a strongly modified up-down asymmetric mode structure, and non-trivial modifications to the eigen-value. Published by AIP Publishing. [<http://dx.doi.org/10.1063/1.5003652>]

I. INTRODUCTION

Even in this era of extensive simulations, linear plasma theory is still important; it provides a benchmark to simulations, and also the mode structure may be used in calculating significant physical quantities such as the Reynolds stress and group velocities. Both of these are, for instance, used in zonal flow studies. It is surprisingly, however, seen that even after 4 decades since the invention of the ballooning theory,^{1–4} constructing a “sound linear theory” for fluctuations in a two-dimensional (2D) tokamak equilibrium still remains a challenge. For example, the so-far most advanced linear theory for kinetic ion temperature gradient (ITG) mode is built on the leading order ballooning equation alone;^{5,6} it has zero Floquet phase.² The class of modes predicted in such a theory, as pointed out in Refs. 7 and 8, form a set of measure zero, and are not generally accessible to realistic plasmas (they were named “isolated modes” in Ref. 9).

From the numerical simulation perspective, the root cause of the difficulty (in constructing a general 2D theory) lies in the unknown 2D boundary condition. For *local* mode (the mode localized around a rational surface like drift wave), it must be a natural boundary condition—that must follow from the physics of the theory, and not merely from a simple-minded intuition.¹⁰ The theory of “isolated mode” was recently advanced in the so-called weakly asymmetric ballooning theory (WABT)^{10,11} based on the Fourier-ballooning transform.⁷ We find that WABT is still poloidally localized (outboard) and has a frequency not too far away from that of the isolated mode (higher growth rate than the general mode). The most important aspect of WABT is that the stringent solvability condition for the isolated mode does

not pertain any longer; it is, in fact, replaced by an easier constraint requirement—the existence of a second small parameter. We would like to mention three distinctions in contrast to the theory of “isolated mode” here. (1) the eigen-values generally deviate from those of isolated mode, as much greater than inverse of toroidal mode number; (2) the 2D physical mode structure is derived, generally up-down asymmetric, and (3) it yields finite Reynolds stress driving toroidal and poloidal rotations, which can be calculated by making use of the obtained mode structure. We believe that all the above mentioned features arise from the translational symmetry breaking (TSB) terms ignored in the higher order theory of the isolated mode.

The generalization of Refs. 11 and 10, however, was so far limited to the fluid models; it is the purpose of this paper to develop a 2D kinetic ballooning theory as exemplified by the ITG model.

The paper is organized as follows. In Sec. II, the 2D gyro-kinetic eigenmode equation for ITG mode is constructed using the Fourier-ballooning transform in an up-down symmetric equilibrium with concentric circular magnetic surfaces. All the trapped ion effects are neglected and velocity variables along unperturbed orbits are assumed to be independent of spatial variables.⁵ The lowest order equation is consistent with the one-dimensional (1D) kinetic equation in Ref. 6, but contains, in addition, a Floquet phase variable. The integral equation will be solved numerically by a spectral method in terms of Weber-Hermite functions. The higher order equation is an ordinary differential equation, containing all TSB terms up to second order, essentially the same form as that presented in Ref. 12. An iterative method is adopted to solve the two equations for the global (Floquet phase independent) eigen-value and 2D mode structure in Sec. III. The global eigenvalue is then compared,

^{a)}Author to whom correspondence should be addressed: xietao@ustc.edu.cn

respectively, with results of 1D gyro-kinetic theory⁶ and a previous 2D fluid theory.¹² The 2D mode structure is also plotted for comparison with that of fluid ITG modes. Major conclusions of this paper are summarized in Sec. IV. Some definitions of symbols in the higher order equation are given in Appendix A. The convergence conditions for wave functions in iteration are discussed in Appendix B.

II. THE WEAKLY UP-DOWN ASYMMETRIC ITG MODE IN THE KINETIC MODEL

In this section, we investigate a non-dissipative kinetic ITG model pertaining to a large-aspect-ratio, up-down symmetric tokamak equilibrium with circular magnetic surfaces. In the toroidal coordinates (r, ϑ, ζ) that corresponding, respectively, to the radial, poloidal, and toroidal directions, the toroidal mode, localized at the rational surface r_j , is represented by

$$\varphi_n(r, \vartheta, \zeta) \equiv \exp(in\zeta - im\vartheta) \sum_l \varphi_l(r) \exp(-il\vartheta), \quad (1)$$

where n is the toroidal mode number, $m = nq(r_j)$ is an integer denoting the poloidal mode number, and the integer l labels the sidebands coupled to the central Fourier mode m .

The 2D Fourier-ballooning transform^{7,13}

$$\varphi_l(x) = \frac{1}{2\pi} \int_{-\pi}^{\pi} d\lambda \int_{-\infty}^{+\infty} dk e^{ik(x-l) - i\lambda l} \varphi(k, \lambda), \quad (2)$$

defines the wave function $\varphi(k, \lambda)$ in the Fourier-ballooning space with $x \equiv nq(r_j)\hat{s}(r - r_j)/r_j$.

One can readily see that the 2D Fourier-ballooning transform is a natural generalization of Lee-Van Dam 1D representation;² the fixed Floquet phase is turned into a variable followed by an integration over the phase variable (phase mixing). The 2D wave function in Fourier-ballooning space, then, obeys

$$\left[L_0 + \frac{iL_1}{n} \frac{\partial}{\partial \lambda} + \frac{L_2}{n^2} \frac{\partial^2}{\partial \lambda^2} + \cdots - \Omega \right] \varphi(k, \lambda) = 0, \quad (3)$$

where $n \equiv |n|$, $(1/n)(\partial/\partial \lambda)$ is asymptotic expansion parameter that results from the TSB terms such as l/m and x/m . In this representation, all terms preserving translational symmetry depend only on the combination $x - l$.

To the lowest order, Eq. (3) is identified to be the standard ballooning equation¹⁰⁻¹²

$$[L_0 - \Omega(\lambda)] \chi(k, \lambda) = 0, \quad (4)$$

where $\chi(k, \lambda)$ is the eigenfunction of the ballooning operator $L_0(k, \lambda)$ associated with local (Floquet phase dependent) eigenvalue $\Omega(\lambda)$; it can be called Floquet-phase parameterized 1D ballooning wave function, since $L_0(k, \lambda)$ does not contain $\partial/\partial \lambda$.

To construct a solvable model, let us assume that the 2D wave function $\varphi(k, \lambda) = \chi(k, \lambda)\psi(\lambda)$, where $\chi(k, \lambda)$ is a slowly varying function of λ while $\partial \ln \psi(\lambda)/\partial \lambda \gg 1$. If n were sufficiently large $[(1/n)(\partial \ln \psi(\lambda)/\partial \lambda) \ll 1]$, then the

equation obeyed by the fastly varying function could be approximated as

$$\left[\frac{d^2}{d\lambda^2} + \frac{in\bar{L}_1}{\bar{L}_2} \frac{d}{d\lambda} + \frac{n^2}{\bar{L}_2} (\Omega(\lambda) - \Omega) \right] \psi(\lambda) = 0, \quad (5)$$

where Ω is the eigenvalue associated with the 2D eigenmode, and $\bar{L}_i \equiv \int_{-\infty}^{\infty} dk \chi^* L_i \chi / \int_{-\infty}^{\infty} dk \chi^* \chi$ ($i = 1, 2$), χ^* is the complex conjugate of χ . It is this global eigenvalue Ω that determines the stability of the mode.

In translating this formalism for the 2D gyro-kinetic ITG eigenmode, we begin with the ion density response, assuming an adiabatic electron response and quasi-neutrality

$$\hat{n}_i(r, \vartheta, \zeta) = -\tau_e \varphi_n(r, \vartheta, \zeta) + \int d^3v J_0(\alpha) h(r, \vartheta, \zeta; v_{\parallel}, v_{\perp}), \quad (6)$$

where $\tau_e \equiv T_e/T_i$, $\alpha \equiv \sqrt{2}k_{\perp} \rho_i \hat{v}_{\perp} = \sqrt{2\tau_e^{-1}k_{\perp} \rho_s \hat{v}_{\perp}}$, $\rho_i \equiv \sqrt{m_i T_i}/eB$, $\rho_s \equiv \sqrt{m_i T_e}/eB$, $\hat{v}_{\perp} \equiv v_{\perp}/v_{ti}$, $v_{ti} \equiv \sqrt{2T_i/m_i}$, $T_e(T_i)$ is the electron (ion) temperature, k_{\perp} is the perpendicular wave number of mode, $\hat{n}_i(r, \vartheta, \zeta)$ is the dimensionless perturbed ion density normalized to equilibrium density, $\varphi_n(r, \vartheta, \zeta)$ is the normalized (to T_e/e) perturbed electrostatic potential, and $J_0(\alpha)$ is the Bessel function of zeroth order. The distribution function $h(r, \vartheta, \zeta; v_{\parallel}, v_{\perp})$ in the non-adiabatic response obeys the gyro-kinetic equation¹⁴

$$\begin{aligned} & (\omega + i\mathbf{v}_{di} \cdot \nabla + iv_{\parallel} \mathbf{b} \cdot \nabla) h(r, \vartheta, \zeta; v_{\parallel}, v_{\perp}) \\ & = F_M(\omega - \hat{\omega}_{*T}) J_0(\alpha) \varphi_n(r, \vartheta, \zeta), \end{aligned} \quad (7)$$

where $\mathbf{v}_{di} \equiv (2T_i/eB)(\mathbf{b} \times \mathbf{\kappa})(\hat{v}_{\perp}^2/2 + \hat{v}_{\parallel}^2)$, \mathbf{b} is the unit vector of magnetic field, $\mathbf{\kappa} \equiv (\mathbf{b} \cdot \nabla)\mathbf{b}$, $\mathbf{b} \cdot \nabla \equiv (1/q(r)R)[\partial/\partial \vartheta + q(r)\partial/\partial \zeta]$, $\hat{\omega}_{*T} = -\tau_e^{-1} \omega_{*e} [1 + \eta_i(\hat{v}_{\perp}^2 + \hat{v}_{\parallel}^2 - 3/2)]$, $\omega_{*e} \equiv nq(r)T_e/eBL_n r$, $F_M \equiv (\pi v_{ti}^2)^{-3/2} \exp(-\hat{v}_{\parallel}^2 - \hat{v}_{\perp}^2)$, $\hat{v}_{\parallel} \equiv v_{\parallel}/v_{ti}$, $k_{\vartheta} \equiv m/r_j$, $L_n \equiv -(d \ln n_i / dr)_r^{-1}$, $L_{T_s} \equiv -(d \ln T_s / dr)_r^{-1}$, $\eta_s \equiv L_n / L_{T_s}$ ($s = i, e$), and ω is the mode frequency. Here, $n_i(r)$ is the plasma density in equilibrium, e is the unit charge, and $B \approx B_0$ and $R \approx R_0$ are the magnetic field and major radius on the magnetic axis, respectively.

Substituting Eq. (1) into Eq. (7) yields

$$\begin{aligned} & \left(\omega - \hat{\omega}_{di} - \frac{v_{\parallel}}{q(r)R} (x - l) \right) h(x, l; v_{\parallel}, v_{\perp}) \\ & = F_M(\omega - \hat{\omega}_{*T}) J_0(\alpha) \varphi_l(x), \end{aligned} \quad (8)$$

where $x \equiv nq(r_j)\hat{s}(r - r_j)/r_j$ is a new radial variable, $\hat{\omega}_{di} \equiv \omega_{di}(\hat{v}_{\perp}^2/2 + \hat{v}_{\parallel}^2)$, $\omega_{di} \varphi_l(x) \equiv (k_{\vartheta} T_i / eBR) \{ [(r_j/r)(1 + l/m) + \hat{s}(\partial/\partial x)] \varphi_{l+1}(x) + [(r_j/r)(1 + l/m) - \hat{s}(\partial/\partial x)] \varphi_{l-1}(x) \}$, $k_{\perp}^2 \rightarrow -k_{\vartheta}^2 [\hat{s}^2 (\partial^2 / \partial x^2) - (r_j/r)^2 (1 + l/m)^2]$, $r_j/r = (1 + x/m\hat{s})^{-1}$.

In Ref. 5, the author directly invoked the existence of a quasi-mode (a typical practice in the literature—generally the ballooning wave function with the Floquet phase specified to be either 0 or π) demanding a zero Floquet phase, and reduced the problem to a single integral ballooning equation, $[L_0 - \Omega(0)] \chi(k, 0) = 0$. The 2D kinetic ballooning theory presented in this paper, however, deals with the second dimension (Floquet phase becoming a variable) squarely; the resulting system consists of two equations: first is the same

ballooning equation parameterized with the Floquet phase [of form Eq. (4)], and the other one is the envelop equation of form Eq. (5).

For independent variables v_{\parallel} and v_{\perp} ,⁵ it is straightforward to cast Eq. (8) into the (k, λ) space by substituting Eq. (2)

$$\begin{aligned} & \left(\omega - \hat{\omega}_{di} - \frac{iv_{\parallel}}{q(r)R} \frac{\partial}{\partial k} \right) h(k, \lambda; v_{\parallel}, v_{\perp}) \\ & = F_M(\omega - \hat{\omega}_{*T}) J_0(\alpha) \varphi(k, \lambda), \end{aligned} \quad (9)$$

where $\omega_{di} \rightarrow (2k_{\perp} T_i / eBR) [(r_j/r)(1 + \lambda) \cos(k + \lambda) + k \hat{s} \sin(k + \lambda)]$, $k_{\perp}^2 \rightarrow k_{\perp}^2 [\hat{s}^2 k^2 + (r_j/r)^2 (1 + \lambda)^2]$ with $\lambda \equiv (-i/m)(\partial/\partial \lambda)$, $r_j/r \rightarrow (1 + \lambda/\hat{s})^{-1}$. In the derivation, use is made of a linear $q(r)$ profile $q(r) := q(r_j) + x/n$, density profile $n_i(r) := n_i(r_j)(1 - t_n x/m)$, and temperature profile $T_s(r) := T_s(r_j)(1 - t_s x/m)$ ($s = i, e$) with $t_n \equiv r_j/\hat{s} L_{n0}$, $t_s \equiv r_j/\hat{s} L_{T_s0}$, $L_{n0} \equiv L_n(r_j) = -(d \ln n_i / dr)_{r_j}^{-1}$, $L_{T_s0} \equiv L_{T_s}(r_j) = -(d \ln T_s / dr)_{r_j}^{-1}$. It is noticeable that the TSB term l/m corresponds to operator $\hat{\lambda}$ in (k, λ) space. The following two rules are helpful to simplify derivation: (a) derivatives act only on wave functions, not on equilibrium quantities; and (b) the TSB term x/m can be replaced by l/m , because of $\partial/\partial \lambda \gg \partial/\partial k$. As a result, the 2D gyro-kinetic ITG eigenmode equation can be written in the form of integral kernel as

$$\int_{-\infty}^{\infty} dk' K(k, k', \lambda, \hat{\lambda}) \varphi(k', \lambda) - \Omega \varphi(k, \lambda) = 0, \quad (10)$$

with

$$\begin{aligned} K(k, k', \lambda, \hat{\lambda}) & = -\frac{i}{\sqrt{\pi}} \frac{(1 + \tau_{e0})}{(1 + \tau_e)} \int_0^{\infty} d\tau \frac{2\sqrt{\nu(\tau)}}{(1 + a_t)} \\ & \times \exp \left[i\omega\tau - a_t \nu(\tau) (k - k')^2 - \frac{\alpha_+}{(1 + a_t)} \right] \\ & \times I_0 \left(\frac{2\alpha_*}{(1 + a_t)} \right) f(k, k', \tau, \hat{\lambda}), \end{aligned} \quad (11)$$

$$\Omega \equiv (1 + \tau_{e0}) \frac{\omega}{\omega_{*e0}}, \quad (12)$$

where

$$\begin{aligned} f(k, k', \tau, \hat{\lambda}) & \equiv \frac{\omega}{\omega_{*e0}} \left\{ \tau_e \omega + \omega_{*e} \left[1 + \eta_i \nu(\tau) (k - k')^2 \right. \right. \\ & \left. \left. - \frac{3\eta_i}{2} \right] + \frac{2\eta_i \omega_{*e}}{(1 + a_t)} \left[1 - \frac{\alpha_+}{(1 + a_t)} \right. \right. \\ & \left. \left. + \frac{2\alpha_*}{(1 + a_t)} \frac{I_1}{I_0} \right] \right\}, \end{aligned} \quad (13)$$

$$a_t \equiv 1 + i\tau \frac{1}{(k - k')} \int_{k'}^k dk'' \omega_{di}, \quad (14)$$

$$\tau \equiv \frac{qR}{v_{ti}} \frac{1}{|\hat{v}_{\parallel}|} \text{sgn}(k - k') (k - k'), \quad (15)$$

$$\nu(\tau) \equiv \frac{q^2 R^2}{v_{ti}^2} \frac{1}{\tau^2}, \quad (16)$$

$$\alpha_+ \equiv \rho_i^2 (k_{\perp}^2 + k'_{\perp}{}^2), \quad \alpha_* \equiv \rho_i^2 k_{\perp} k'_{\perp}, \quad (17)$$

where quantities with subscript “0” stand for the quantity at rational surface, $I_0(I_1)$ is the zeroth (first) order modified Bessel function.

In order to describe contributions from TSB terms, we perform Taylor expansion around the rational surface r_j on the integral kernel Eq. (11) to the second order with respect to $\hat{\lambda}$. It yields

$$L_0 \chi(k, \lambda) = \int_{-\infty}^{\infty} dk' K(k, k', \lambda, 0) \chi(k', \lambda), \quad (18)$$

$$\bar{L}_1(\lambda) = -\frac{1}{q_0} \frac{\int_{-\infty}^{\infty} dk \chi^*(k, \lambda) \int_{-\infty}^{\infty} dk' \frac{dK}{d\lambda} \Big|_{\lambda=0} \chi(k', \lambda)}{\int_{-\infty}^{\infty} dk \chi^*(k, \lambda) \chi(k, \lambda)}, \quad (19)$$

$$\bar{L}_2(\lambda) = -\frac{1}{2q_0^2} \frac{\int_{-\infty}^{\infty} dk \chi^*(k, \lambda) \int_{-\infty}^{\infty} dk' \frac{d^2 K}{d\lambda^2} \Big|_{\lambda=0} \chi(k', \lambda)}{\int_{-\infty}^{\infty} dk \chi^*(k, \lambda) \chi(k, \lambda)}, \quad (20)$$

where

$$\begin{aligned} K(k, k', \lambda, 0) & = -\frac{i}{\sqrt{\pi}} \int_0^{\infty} d\tau_0 \frac{2\sqrt{\nu_0}}{(1 + a_{t0})} \\ & \times \exp \left[i\omega\tau_0 - a_{t0} \nu_0 (k - k')^2 - \frac{\alpha_{+0}}{(1 + a_{t0})} \right] \\ & \times I_0 \left(\frac{2\alpha_{*0}}{(1 + a_{t0})} \right) f(k, k', \tau_0, 0), \end{aligned} \quad (21)$$

$$\begin{aligned} f(k, k', \tau_0, 0) & \equiv \frac{\omega}{\omega_{*e0}} \left\{ \tau_{e0} \omega + \omega_{*e0} \left[1 + \eta_{i0} \nu_0 (k - k')^2 \right. \right. \\ & \left. \left. - \frac{3\eta_{i0}}{2} \right] + \frac{2\eta_{i0} \omega_{*e0}}{(1 + a_{t0})} \left[1 - \frac{\alpha_{+0}}{(1 + a_{t0})} \right. \right. \\ & \left. \left. + \frac{2\alpha_{*0}}{(1 + a_{t0})} \frac{I_1}{I_0} \right] \right\}, \end{aligned} \quad (22)$$

$$\begin{aligned} \frac{dK}{d\lambda} \Big|_{\lambda=0} & = -\frac{i}{\sqrt{\pi}} \int_0^{\infty} d\tau_0 G(k, k', \tau_0) \frac{2\sqrt{\nu_0}}{(1 + a_{t0})} \\ & \times \exp \left[i\omega\tau_0 - a_{t0} \nu_0 (k - k')^2 - \frac{\alpha_{+0}}{(1 + a_{t0})} \right] \\ & \times I_0 \left(\frac{2\alpha_{*0}}{(1 + a_{t0})} \right), \end{aligned} \quad (23)$$

$$\begin{aligned} \frac{d^2 K}{d\lambda^2} \Big|_{\lambda=0} & = -\frac{i}{\sqrt{\pi}} \int_0^{\infty} d\tau_0 H(k, k', \tau_0) \frac{2\sqrt{\nu_0}}{(1 + a_{t0})} \\ & \times \exp \left[i\omega\tau_0 - a_{t0} \nu_0 (k - k')^2 - \frac{\alpha_{+0}}{(1 + a_{t0})} \right] \\ & \times I_0 \left(\frac{2\alpha_{*0}}{(1 + a_{t0})} \right). \end{aligned} \quad (24)$$

We notice that when $\lambda = 0$ the ballooning equation is consistent with Eq. (11) in Ref. 6. The higher order equation is found to have the same form as derived in Ref. 12. However,

Eqs. (19) and (20) can only be calculated by resorting to numerical integration, which will be introduced in detail in Sec. III. In order to improve the readability, the definitions of $G(k, k', \tau_0)$ and $H(k, k', \tau_0)$ will be given in Appendix A.

III. NUMERICAL RESULTS

An iterative integral code named KITG-WABT has been developed to solve the system consisting of the integral equation (4), and the differential equation (5). Equation (4) was solved numerically using the spectral method. The base functions are chosen to be Weber-Hermite functions, Hermite polynomials with a weight function $\exp(-k^2/2)$. The ballooning wave function, then, is approximated by

$$\chi(k, \lambda) \approx \sum_{i=0}^N A_i(\lambda) H_i(k) \exp(-k^2/2), \quad (25)$$

where $H_i(k)$ is the Hermite polynomial of degree i , $A_i(\lambda)$ is the undetermined coefficient only related to λ .

After multiplying by $H_j(k) \exp(-k^2/2)$ ($j = 0, 1, \dots, N$) and integrating over k , Eq. (4) [with Eq. (18)] converts to a system of linear algebraic equations

$$[\mathbf{M} - \Omega(\lambda)\mathbf{I}]\mathbf{A} = 0, \quad (26)$$

where $\mathbf{A} \equiv (A_0, A_1, \dots, A_N)^T$, \mathbf{M} is a $(N+1) \times (N+1)$ dimensional matrix, and \mathbf{I} is an unit matrix. The integrations over τ and k' are performed with a Gaussian rule of even order. The integration over k is carried out with a trapezoidal rule. The same numerical integral scheme is also used to calculate $\bar{L}_1(\lambda)$ and $\bar{L}_2(\lambda)$.

Since the matrix \mathbf{M} depends on the mode frequency ω , Eq. (26) needs to be solved numerically using an iterative method. The concrete procedure is briefly described as follows. (1) An initial guess, $\omega^{(0)}$, is substituted into the coefficient matrix \mathbf{M} to solve Eq. (26) for $\Omega(\lambda)$ using the QR decomposition technique.¹⁵ (2) The inverse power method is adopted to obtain \mathbf{A} and $\chi(k, \lambda)$. (3) $\chi(k, \lambda)$ is substituted into Eqs. (19) and (20) for $\bar{L}_1(\lambda)$ and $\bar{L}_2(\lambda)$. (4) Then, we make use of the shooting method to solve Eq. (5) for the global eigenvalue $\Omega^{(1)}$. (5) $\Omega^{(1)}$ is substituted into Eq. (12) for $\omega^{(1)}$. (6) Repeat the steps (1)–(5) with $\omega^{(0)}$ replaced by $\omega^{(1)}$ until the convergence condition $|1 - \omega^{(i+1)}/\omega^{(i)}| < 10^{-4}$ is satisfied. The corresponding convergence condition for wave functions $|\varphi_0(x)|$ (the wave function in (x, l) representation with $l = 0$) is found to be $|1 - |\varphi_0(x)|^{(i+1)}/|\varphi_0(x)|^{(i)}| \approx 5 \times 10^{-4}$; it will be further described in Appendix B.

The physical parameters, chosen here, corresponding to the operating conditions on HL-2A ($R = 1.65$ m, $a = 0.4$ m, $T_{e0} = T_{i0} = 250$ eV, $B = 1.35$ T),¹⁶ are $k_{\vartheta}\rho_{s0} = -0.53$, $\hat{s} = 1$, $q_0 = 2$, $\eta_{i0} = \eta_{e0} = 3.5$, $L_{n0}/R = 0.12$, and $r_j/a = 0.6$. The corresponding toroidal mode number is $n = -53$.

In Figs. 1(a)–1(d), the ballooning wave function $\chi(k, \lambda)$ is plotted versus k for $\lambda = 0, \pi/4, \pi/2$, and $-\pi/2$ (with $N = 10$); the blue and red lines denote the real and imaginary parts. The corresponding local eigenvalues are listed in

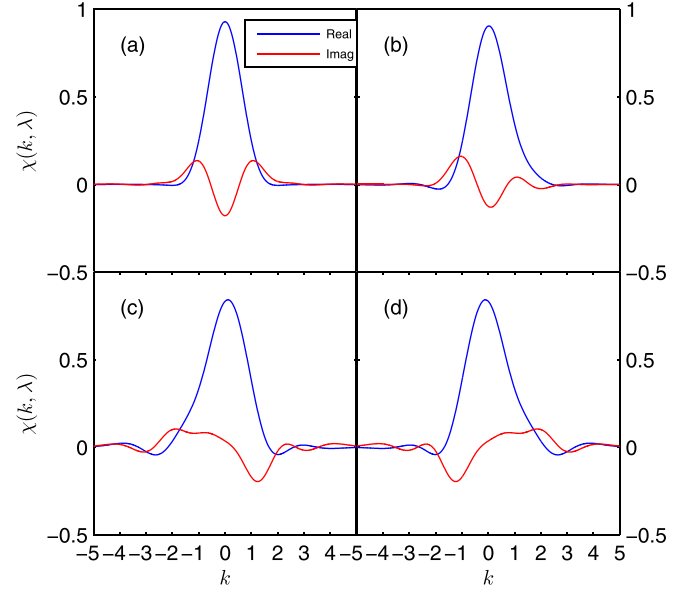


FIG. 1. The real (blue line) and imaginary (red line) parts of ballooning wave functions $\chi(k, \lambda)$ versus k for (a) $\lambda = 0$; (b) $\lambda = \pi/4$; (c) $\lambda = \pi/2$; (d) $\lambda = -\pi/2$. The physical parameters are $k_{\vartheta}\rho_{s0} = -0.53$, $\hat{s} = 1$, $q_0 = 2$, $\eta_{i0} = \eta_{e0} = 3.5$, $L_{n0}/R = 0.12$, and $n = -53$.

Table I. The local eigenvalue at $\lambda = 0$, $\omega(\lambda = 0)/|\omega_{*e0}| = -0.42 + 0.42i$, is consistent with Ref. 6. The global eigenvalue is iteratively calculated to be $\omega/|\omega_{*e0}| = -0.40 + 0.34i$ with a growth rate obviously smaller than the local one at $\lambda = 0$.

In order to compare with the weakly up-down asymmetric ITG mode based on the 2D fluid model,¹² another set of parameters is chosen: $k_{\vartheta}\rho_{s0} = -0.51$, $\hat{s} = 0.9$, $q_0 = 1.7$, $\eta_{i0} = \eta_{e0} = 3$, and $L_{n0}/R = 0.1$. The rest of the parameters are the same as those used in Fig. 1. The corresponding toroidal mode number is $n = -60$. The global eigenvalues, $\omega/|\omega_{*e0}| = -0.27 + 0.28i$ for the gyro-kinetic, and $\omega/|\omega_{*e0}| = -0.25 + 0.83i$ for the fluid model, show that the fluid model greatly overestimates the growth rate.

The real (blue) and imaginary (red) parts of the envelop function $\psi(\lambda)$ are plotted in Fig. 2. It is found that the deviation of peak in $\psi(\lambda)$ from $\lambda = 0$ is greater than the result obtained in the fluid model.¹²

The 2D mode structure is shown in Fig. 3 via the contour plot of $\text{Re}[\varphi_n(r, \vartheta, 0)]$. The radial position is determined by the mapping $(1 + x/m\hat{s})(r_j/a)$. The up-down asymmetry of the mode structure is shown to be obviously stronger than that of 2D fluid model.¹² It is expected that the weakly up-down asymmetric kinetic ITG mode can provide torque for intrinsic rotation comparable to that of the

TABLE I. The local eigenvalues corresponding to the ballooning wave functions as displayed in Figs. 1(a)–1(d).

λ	$\omega(\lambda)/ \omega_{*e0} $
0	$-0.42 + 0.42i$
$\pi/4$	$-0.32 + 0.37i$
$\pm\pi/2$	$-0.19 + 0.13i$

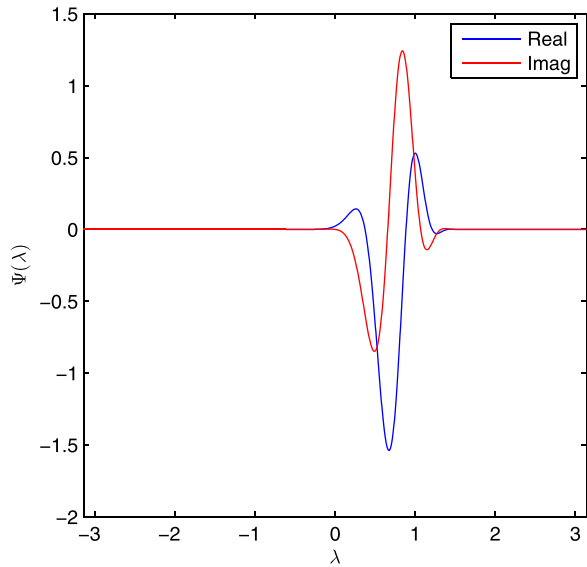


FIG. 2. The real (blue line) and imaginary (red line) parts of envelop function $\psi(\lambda)$ versus λ .

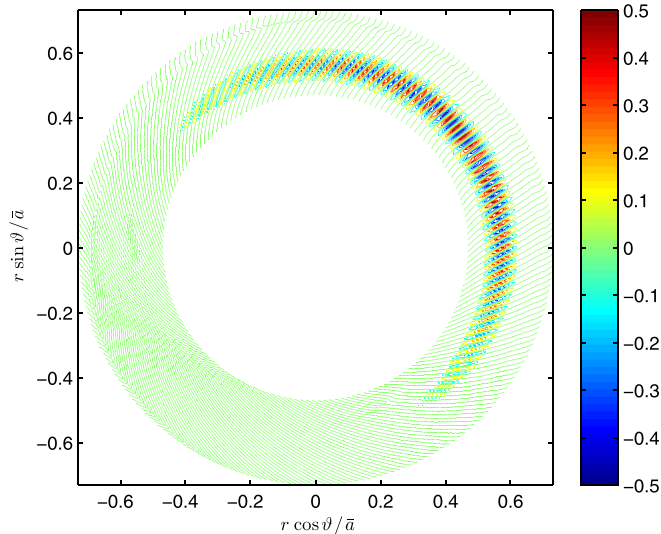


FIG. 3. Level contours of the real parts of the 2D mode structure on a poloidal cross section.

2D fluid mode, even though its growth rate is smaller than the latter.

To conclude this section, we should mention that construction of the higher order theory for WABT requires a second small parameter $\Xi \equiv \bar{L}_1(\lambda_*)/2\bar{L}_2(\lambda_*)$ with λ_* representing the localization of $\psi(\lambda)$ in λ .^{10,11} The physics parameters used in the present paper were chosen to lie in the region of validity. In particular, Ξ is found to be less than 1/3, even though the tilt of the ballooning orientation (Fig. 3) may give a different impression.

IV. SUMMARY

The 2D kinetic ballooning theory for the gyro-kinetic ITG model, developed in this paper, provides the full mode structure localized at the given rational surface (shown in Fig. 3); it also predicts a global eigenvalue (-0.40

+0.34*i*) somewhat different from the local eigen-value ($-0.42 + 0.42i$) calculated, conventionally, at $\lambda = 0$. The lower growth rate from the 2D kinetic model may be attributed to finite deviation of the envelop peak away from the equatorial plane.

The ballooning theory, as an asymptotic theory, is not expected to be able to make very accurate predictions. We contend, however, that its use best should be in providing natural boundary conditions for local modes in a tokamak. For example, it would make sense to take the asymptotic results of the kinetic ballooning theory as the natural boundary condition for certain gyro-kinetic simulation, such as routinely done via a code like GENE;^{17,18} we believe that it will be better than using the flux tube boundary condition based on the quasi-mode.

The Reynolds stress induced by the 2D gyro-kinetic ITG mode can readily be calculated as was done for the fluid ITG.¹²

ACKNOWLEDGMENTS

This research was supported by the Key Research Program of Frontier Sciences CAS (QZDB-SSWSYS004), National Magnetic Confinement Fusion Energy Research Project (2015GB104004, 2015GB111003), National Natural Science Foundation of China (NSFC-11575185, 11575186), by the U.S. Department of Energy Grant No. DE-FG02-04ER-54742, by Foundation of Sichuan University of Science and Engineering Grant No. 2016RCL21, by Scientific Research Fund of the Sichuan Provincial Education Department Grant No. 17ZA0281, by National Magnetic Confinement Fusion Science Program under Grant No. 2013GB112009, and by Sichuan University of Science and Engineering High Performance Computing Center provided computational.

APPENDIX A: SOME DEFINITIONS IN THE HIGHER ORDER EQUATION

In Eqs. (23) and (24), $G(k, k', \tau_0)$ and $H(k, k', \tau_0)$ are defined as

$$G(k, k', \tau_0) \equiv h'(k, k', \tau_0)f(k, k', \tau_0, 0) + f'(k, k', \tau_0, 0), \quad (\text{A1})$$

$$H(k, k', \tau_0) \equiv \left[g(k, k', \tau_0) + h'^2(k, k', \tau_0) \right] f(k, k', \tau_0, 0) + 2h'(k, k', \tau_0)f'(k, k', \tau_0, 0) + f''(k, k', \tau_0, 0), \quad (\text{A2})$$

where

$$h'(k, k', \tau_0) \equiv \frac{1}{\tau_0} \frac{d\tau}{d\lambda} - \frac{1}{(1 + \tau_{e0})} \frac{d\tau_e}{d\lambda} - \frac{1}{(1 + a_{r0})} \frac{da_r}{d\lambda} - \nu_0(k - k')^2 \frac{da_t}{d\lambda} + i\omega \frac{d\tau}{d\lambda} - \frac{d}{d\lambda} \frac{\alpha_+}{(1 + a_t)} + \frac{I_1}{I_0} \frac{d}{d\lambda} \frac{2\alpha_*}{(1 + a_t)}, \quad (\text{A3})$$

$$f'(k, k', \tau_0, 0) \equiv \frac{\omega}{\omega_{*e0}} \left\{ \omega \frac{d\tau_e}{d\lambda} + \frac{d\omega_{*e}}{d\lambda} \left[1 + \eta_{i0}\nu_0(k - k')^2 - \frac{3\eta_{i0}}{2} \right] + \omega_{*e0} \frac{d\eta_i}{d\lambda} \left[\nu_0(k - k')^2 - \frac{3}{2} \right] \right. \\ \left. - \frac{2\eta_{i0}\omega_{*e0}}{(1 + a_{i0})^2} \frac{da_t}{d\lambda} \left[1 - \frac{\alpha_{+0}}{(1 + a_{i0})} + \frac{2\alpha_{*0}}{(1 + a_{i0})} \frac{I_1}{I_0} \right] + \frac{2}{(1 + a_{i0})} \frac{d(\eta_i\omega_{*e})}{d\lambda} \left[1 - \frac{\alpha_{+0}}{(1 + a_{i0})} + \frac{2\alpha_{*0}}{(1 + a_{i0})} \frac{I_1}{I_0} \right] \right. \\ \left. + \frac{2\eta_{i0}\omega_{*e0}}{(1 + a_{i0})} \left[-\frac{d}{d\lambda} \frac{\alpha_{+}}{(1 + a_t)} + \frac{2\alpha_{*0}}{(1 + a_{i0})} \left(1 - \frac{I_1^2}{I_0^2} \right) \frac{d}{d\lambda} \frac{2\alpha_{*}}{(1 + a_t)} \right] \right\}, \tag{A4}$$

$$g(k, k', \tau_0) \equiv \frac{1}{\tau_0} \frac{d^2\tau}{d\lambda^2} - \frac{1}{\tau_0^2} \left(\frac{d\tau}{d\lambda} \right)^2 - \frac{1}{(1 + \tau_{e0})} \left[\frac{d^2\tau_e}{d\lambda^2} - \frac{1}{(1 + \tau_{e0})} \left(\frac{d\tau_e}{d\lambda} \right)^2 \right] - \frac{1}{(1 + a_{i0})} \left[\frac{d^2a_t}{d\lambda^2} - \frac{1}{(1 + a_{i0})} \left(\frac{da_t}{d\lambda} \right)^2 \right] \\ - \nu_0(k - k')^2 \frac{d^2a_t}{d\lambda^2} + i\omega \frac{d^2\tau}{d\lambda^2} - \frac{d^2}{d\lambda^2} \frac{\alpha_{+}}{(1 + a_t)} + \frac{d}{d\lambda} \left(\frac{I_1}{I_0} \frac{d}{d\lambda} \frac{2\alpha_{*}}{(1 + a_t)} \right), \tag{A5}$$

$$f''(k, k', \tau_0, 0) \equiv \frac{\omega}{\omega_{*e0}} \left\{ \omega \frac{d^2\tau_e}{d\lambda^2} + \frac{d^2\omega_{*e}}{d\lambda^2} \left[1 + \eta_{i0}\nu_0(k - k')^2 - \frac{3\eta_{i0}}{2} \right] + 2 \frac{d\omega_{*e}}{d\lambda} \frac{d\eta_i}{d\lambda} \left[\nu_0(k - k')^2 - \frac{3}{2} \right] \right. \\ \left. + \frac{d^2\eta_i}{d\lambda^2} \left[\nu_0(k - k')^2 - \frac{3}{2} \right] + \frac{4}{(1 + a_{i0})} \frac{d(\eta_i\omega_{*e})}{d\lambda} \left[-\frac{d}{d\lambda} \frac{\alpha_{+}}{(1 + a_t)} + \frac{2\alpha_{*0}}{(1 + a_{i0})} \left(1 - \frac{I_1^2}{I_0^2} \right) \frac{d}{d\lambda} \frac{2\alpha_{*}}{(1 + a_t)} \right] \right. \\ \left. - \frac{2\eta_{i0}\omega_{*e0}}{(1 + a_{i0})^2} \frac{d^2a_t}{d\lambda^2} \left[1 - \frac{\alpha_{+0}}{(1 + a_{i0})} + \frac{2\alpha_{*0}}{(1 + a_{i0})} \frac{I_1}{I_0} \right] - \frac{4\eta_{i0}\omega_{*e0}}{(1 + a_{i0})^2} \frac{da_t}{d\lambda} \left[-\frac{d}{d\lambda} \frac{\alpha_{+}}{(1 + a_t)} + \frac{2\alpha_{*0}}{(1 + a_{i0})} \left(1 - \frac{I_1^2}{I_0^2} \right) \frac{d}{d\lambda} \frac{2\alpha_{*}}{(1 + a_t)} \right] \right. \\ \left. - \frac{4}{(1 + a_{i0})^2} \frac{da_t}{d\lambda} \frac{d(\eta_i\omega_{*e})}{d\lambda} \left[1 - \frac{\alpha_{+0}}{(1 + a_{i0})} + \frac{2\alpha_{*0}}{(1 + a_{i0})} \frac{I_1}{I_0} \right] + \frac{2}{(1 + a_{i0})} \frac{d^2(\eta_i\omega_{*e})}{d\lambda^2} \left[1 - \frac{\alpha_{+0}}{(1 + a_{i0})} + \frac{2\alpha_{*0}}{(1 + a_{i0})} \frac{I_1}{I_0} \right] \right. \\ \left. + \frac{4\eta_{i0}\omega_{*e0}}{(1 + a_{i0})^3} \left(\frac{da_t}{d\lambda} \right)^2 \left[1 - \frac{\alpha_{+0}}{(1 + a_{i0})} + \frac{2\alpha_{*0}}{(1 + a_{i0})} \frac{I_1}{I_0} \right] + \frac{4\eta_{i0}\omega_{*e0}\alpha_{*0}}{(1 + a_{i0})^2} \left(1 - \frac{I_1^2}{I_0^2} \right) \frac{d^2}{d\lambda^2} \frac{2\alpha_{*}}{(1 + a_t)} \right. \\ \left. + \frac{2\eta_{i0}\omega_{*e0}}{(1 + a_{i0})} \left[-\frac{d^2}{d\lambda^2} \frac{\alpha_{+}}{(1 + a_t)} + \left(1 - \frac{I_1^2}{I_0^2} \right) \left(\frac{d}{d\lambda} \frac{2\alpha_{*}}{(1 + a_t)} \right)^2 + \frac{2\alpha_{*0}}{(1 + a_{i0})} \frac{I_1}{I_0} \left(\frac{2I_1^2}{I_0^2} - \frac{I_2}{I_0} - 1 \right) \left(\frac{d}{d\lambda} \frac{2\alpha_{*}}{(1 + a_t)} \right)^2 \right] \right\}, \tag{A6}$$

with

$$\frac{d\tau}{d\lambda} = \tau_0 \left(1 + \frac{1}{2} t_{Ti} \right), \quad \frac{d\tau_e}{d\lambda} = \tau_{e0} (t_{Ti} - t_{Te}), \tag{A7}$$

$$\frac{da_t}{d\lambda} = -\frac{2i\tau_{e0}^{-1}\tau_0\epsilon_{n0}}{(k - k')} \left\{ [\sin(k + \lambda) - \sin(k' + \lambda)] \left[2 + \hat{s} - \frac{1}{\hat{s}} - \frac{1}{2} t_{Ti} (1 + \hat{s}) \right] - \hat{s} [k \cos(k + \lambda) - k' \cos(k' + \lambda)] \left(1 - \frac{1}{2} t_{Ti} \right) \right\}, \tag{A8}$$

$$\frac{d\omega_{*e}}{d\lambda} = \omega_{*e0} \left[\left(1 - \frac{1}{\hat{s}} \right) - t_n (\eta_{e0} - 1) \right], \quad \frac{d\eta_i}{d\lambda} = t_n \eta_{i0} (\eta_{i0} - 1), \tag{A9}$$

$$\frac{d(\eta_i\omega_{*e})}{d\lambda} = \eta_{i0}\omega_{*e0} \left[\left(1 - \frac{1}{\hat{s}} \right) + t_n (\eta_{i0} - \eta_{e0}) \right], \tag{A10}$$

$$\frac{d\alpha_{+}}{d\lambda} = \tau_{e0}^{-1} k_{\parallel}^2 \rho_{s0}^2 \left[4 \left(1 - \frac{1}{\hat{s}} \right) - t_{Ti} (2 + \hat{s}^2 k^2 + \hat{s}^2 k'^2) \right], \tag{A11}$$

$$\frac{d\alpha_{*}}{d\lambda} = \tau_{e0}^{-1} k_{\parallel}^2 \rho_{s0}^2 \sqrt{(1 + \hat{s}^2 k^2)(1 + \hat{s}^2 k'^2)} \left[\frac{1}{(1 + \hat{s}^2 k^2)} \left(1 - \frac{1}{\hat{s}} \right) + \frac{1}{(1 + \hat{s}^2 k'^2)} \left(1 - \frac{1}{\hat{s}} \right) - t_{Ti} \right], \tag{A12}$$

$$\frac{d}{d\lambda} \frac{\alpha_{+}}{(1 + a_t)} = \frac{1}{(1 + a_{i0})} \left[\frac{d\alpha_{+}}{d\lambda} - \frac{\alpha_{+0}}{(1 + a_{i0})} \frac{da_t}{d\lambda} \right], \tag{A13}$$

$$\frac{d}{d\lambda} \frac{2\alpha_{*}}{(1 + a_t)} = \frac{2}{(1 + a_{i0})} \frac{d\alpha_{*}}{d\lambda} - \frac{2\alpha_{*0}}{(1 + a_{i0})^2} \frac{da_t}{d\lambda}, \tag{A14}$$

$$\frac{d^2\tau}{d\lambda^2} = t_{Ti} \left(1 + \frac{3}{4} t_{Ti} \right), \quad \frac{d^2\tau_e}{d\lambda^2} = 2\tau_{e0} t_{Ti} (t_{Ti} - t_{Te}), \tag{A15}$$

$$\begin{aligned} \frac{d^2 a_t}{d\lambda^2} = & -\frac{2i\tau_{e0}^{-1}\tau_0\epsilon_{n0}}{(k-k')} \left\{ [\sin(k+\lambda) - \sin(k'+\lambda)] \right. \\ & \times \left[2\left(1 - \frac{1}{\hat{s}}\right)^2 - t_{Ti}\left(2 + \hat{s} - \frac{1}{\hat{s}}\right) - \frac{1}{4}t_{Ti}^2(1 + \hat{s}) \right] \\ & \left. + \hat{s}[k \cos(k+\lambda) - k' \cos(k'+\lambda)]t_{Ti}\left(1 + \frac{1}{4}t_{Ti}\right) \right\}, \end{aligned} \quad (\text{A16})$$

$$\begin{aligned} \frac{d^2 \omega_{*e}}{d\lambda^2} = & -2\omega_{*e0} \left[\frac{1}{\hat{s}}\left(1 - \frac{1}{\hat{s}}\right) + t_n(\eta_{e0} - 1)\left(1 - \frac{1}{\hat{s}}\right) \right. \\ & \left. + t_n^2(\eta_{e0} - 1) \right], \end{aligned} \quad (\text{A17})$$

$$\frac{d^2 \eta_i}{d\lambda^2} = 2\eta_{i0}t_n t_{Ti}(\eta_{i0} - 1), \quad (\text{A18})$$

$$\begin{aligned} \frac{d^2(\eta_i \omega_{*e})}{d\lambda^2} = & 2\eta_{i0}\omega_{*e0} \left[-\frac{1}{\hat{s}}\left(1 - \frac{1}{\hat{s}}\right) + t_n(\eta_{i0} - \eta_{e0}) \right. \\ & \left. \times \left(1 - \frac{1}{\hat{s}}\right) + t_n^2\eta_{i0}(\eta_{i0} - \eta_{e0}) \right], \end{aligned} \quad (\text{A19})$$

$$\frac{d^2 \alpha_+}{d\lambda^2} = 4\tau_{e0}^{-1}k_{\parallel}^2\rho_{s0}^2\left(1 - \frac{1}{\hat{s}}\right)\left(1 - \frac{3}{\hat{s}} - 2t_{Ti}\right), \quad (\text{A20})$$

$$\begin{aligned} \frac{d^2 \alpha_*}{d\lambda^2} = & \tau_{e0}^{-1}k_{\parallel}^2\rho_{s0}^2\sqrt{(1 + \hat{s}^2k^2)(1 + \hat{s}^2k'^2)}\left(1 - \frac{1}{\hat{s}}\right) \\ & \times \left\{ \left(1 - \frac{3}{\hat{s}} - 2t_{Ti}\right) \left[\frac{1}{(1 + \hat{s}^2k^2)} + \frac{1}{(1 + \hat{s}^2k'^2)} \right] \right. \\ & \left. - \left(1 - \frac{1}{\hat{s}}\right) \left[\frac{1}{(1 + \hat{s}^2k^2)} - \frac{1}{(1 + \hat{s}^2k'^2)} \right]^2 \right\}, \end{aligned} \quad (\text{A21})$$

$$\begin{aligned} \frac{d^2}{d\lambda^2} \frac{\alpha_+}{(1 + a_t)} = & \frac{1}{(1 + a_{t0})} \left[\frac{d^2 \alpha_+}{d\lambda^2} - \frac{\alpha_{+0}}{(1 + a_{t0})} \frac{d^2 a_t}{d\lambda^2} \right. \\ & \left. - \frac{2}{(1 + a_{t0})} \frac{d\alpha_+}{d\lambda} \frac{da_t}{d\lambda} + \frac{2\alpha_{+0}}{(1 + a_{t0})^2} \left(\frac{da_t}{d\lambda} \right)^2 \right], \end{aligned} \quad (\text{A22})$$

$$\begin{aligned} \frac{d^2}{d\lambda^2} \frac{2\alpha_*}{(1 + a_t)} = & \frac{2}{(1 + a_{t0})} \left[\frac{d^2 \alpha_*}{d\lambda^2} - \frac{\alpha_{*0}}{(1 + a_{t0})} \frac{d^2 a_t}{d\lambda^2} \right. \\ & \left. - \frac{2}{(1 + a_{t0})} \frac{d\alpha_*}{d\lambda} \frac{da_t}{d\lambda} + \frac{2\alpha_{*0}}{(1 + a_{t0})^2} \left(\frac{da_t}{d\lambda} \right)^2 \right], \end{aligned} \quad (\text{A23})$$

$$\begin{aligned} \frac{d}{d\lambda} \left[\frac{I_1}{I_0} \frac{d}{d\lambda} \frac{2\alpha_*}{(1 + a_t)} \right] = & \frac{1}{2} \left(1 + \frac{I_2}{I_0} - \frac{2I_1^2}{I_0^2} \right) \left[\frac{d}{d\lambda} \frac{2\alpha_*}{(1 + a_t)} \right]^2 \\ & + \frac{I_1}{I_0} \frac{d^2}{d\lambda^2} \frac{2\alpha_*}{(1 + a_t)}, \end{aligned} \quad (\text{A24})$$

where the quantities with subscript “0” indicate the value on the rational surface r_j , I_2 is the modified Bessel function of second order.

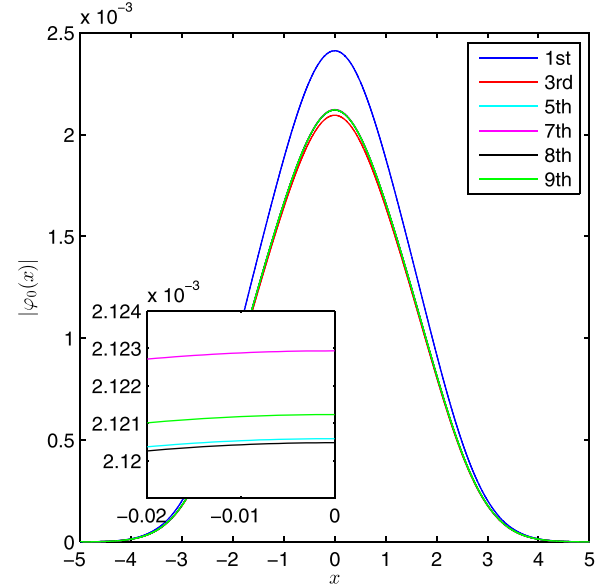


FIG. 4. The wave functions in iteration $|\varphi_0(x)|^{(i)}$ for the same parameters as in Fig. 1. The sequence numbers of iteration (i) are shown in the legend.

APPENDIX B: THE CONVERGENCE CONDITION OF WAVE FUNCTIONS

As displayed in Fig. 4, we give the radial variations of wave functions in iteration $|\varphi_0(x)|^{(i)}$ for the same parameters as in Fig. 1. $\varphi_0(x)$ represents $l = 0$ component of $\varphi_l(x)$ and the superscript (i) stands for the sequence numbers of iteration. The close-up view of wave functions near to $x = 0$ is also shown using picture-in-picture. It is obvious that the wave functions tend to be convergent with the increasing of iterations. In contrast to the required convergence condition of eigenvalue ($< 10^{-4}$), the maximum relative difference of $|\varphi_0(x)|$ is 5×10^{-4} (taken from the 8th to 9th iterations).

¹J. W. Connor, R. J. Hastie, and J. B. Taylor, *Phys. Rev. Lett.* **40**, 396 (1978).

²Y. C. Lee and J. W. Van Dam, in *Proceedings of the Finite Beta Theory Workshop, Varenna Summer School of Plasma Physics, September 1977, Varenna, Italy*, edited by B. Coppi and B. Sadowski (U.S. Department of Energy, Office of Fusion Energy, Washington DC, 1979), CONF-7709167, p. 93.

³A. H. Glasser, in *Proceedings of the Finite Beta Theory Workshop, Varenna Summer School of Plasma Physics, September 1977, Varenna, Italy*, edited by B. Coppi and B. Sadowski (U.S. Department of Energy, Office of Fusion Energy, Washington DC, 1979), CONF-7709167, p. 55.

⁴F. Pegoraro and T. Schep, in *Seventh Conference on Plasma Physics and Controlled Nuclear Fusion Research, Innsbruck, August 1978 paper IAEACN-37/F-5, International Conference on Plasma Physics and Controlled Nuclear Fusion Research 1978, 1* (International Atomic Energy Agency, Vienna, 1979).

⁵F. Romanelli, *Phys. Fluids B* **1**, 1018 (1989).

⁶J. Q. Dong, W. Horton, and J. Y. Kim, *Phys. Fluids B* **4**, 1867 (1992).

⁷Y. Z. Zhang and S. M. Mahajan, *Phys. Lett. A* **157**, 133 (1991).

⁸D. Dickinson, C. M. Roach, J. M. Skipp, and H. R. Wilson, *Phys. Plasmas* **21**, 010702 (2014).

⁹J. B. Taylor, H. R. Wilson, and J. W. Connor, *Plasma Phys. Controlled Fusion* **38**, 243 (1996).

¹⁰T. Xie, H. Qin, Y. Z. Zhang, and S. M. Mahajan, *Phys. Plasmas* **23**, 042514 (2016).

¹¹Y. Z. Zhang and T. Xie, *Nucl. Fusion Plasma Phys.* **33**, 193 (2013) (in Chinese with English abstract).

¹²T. Xie, Y. Z. Zhang, S. M. Mahajan, Z. Y. Liu, and H. He, *Phys. Plasmas* **23**, 102313 (2016).

- ¹³Y. Z. Zhang, S. M. Mahajan, and X. D. Zhang, *Phys. Fluids B* **4**, 2729 (1992).
- ¹⁴P. J. Catto, *Plasma Phys.* **20**, 719 (1978).
- ¹⁵J. Stoer and R. Bulirsch, *Introduction to Numerical Analysis*, 2nd ed. (Springer-Verlag New York, Inc., New York, NY, 2002), Sec. 6.6, p. 370.
- ¹⁶D. L. Yu, Y. L. Wei, L. Liu, J. Q. Dong, K. Ida, K. Itoh, A. P. Sun, J. Y. Cao, Z. B. Shi, Z. X. Wang, Y. Xiao, B. S. Yuan, H. R. Du, X. X. He, W. J. Chen, Q. Ma, S.-I. Itoh, K. J. Zhao, Y. Zhou, J. Wang, X. Q. Ji, W. L. Zhong, Y. G. Li, J. M. Gao, W. Deng, Y. Liu, Y. Xu, L. W. Yan, Q. W. Yang, X. T. Ding, X. R. Duan, Y. Liu, and HL-2A Team, *Nucl. Fusion* **56**, 056003 (2016).
- ¹⁷F. Jenko, W. Dorland, M. Kotschenreuther, and B. N. Rogers, *Phys. Plasmas* **7**, 1904 (2000).
- ¹⁸T. Görler, X. Lapillonne, S. Brunner, T. Dannert, F. Jenko, F. Merz, and D. Told, *J. Comput. Phys.* **230**, 7053 (2011).